Available online at www.sciencedirect.com
SCIENCE DIRECT®
Spectrochimica Acta Part A 61 (2005) 3117–3123
SPECTROCHIMICA ACTA PART A
www.elsevier.com/locate/saa

Theoretical and experimental study on formation and adsorption of enolic species on Ag-Pd/Al_2O_3 catalyst

Hongwei Gao, Hong He*, Qingcai Feng, Jin Wang

State Key Laboratory of Environmental Chemistry and Ecotoxicology, Chinese Academy of Sciences, Beijing 100085, China

Received 28 October 2004; received in revised form 24 November 2004; accepted 26 November 2004

Abstract

The formation and adsorption of enolic species on a palladium promoted Ag/Al_2O_3 catalyst (denoted Ag-Pd/Al_2O_3) during the selective catalytic reduction (SCR) of NO_x by C_3H_6 has been studied by means of DRIFTS and density functional calculations. The structure of the enolic species adsorbed on Ag-Pd/Al_2O_3 catalyst has been established based on the in situ DRIFTS spectra and simulated results. The reaction mechanism from C_3H_6 to enolic species on Ag-Pd/Al_2O_3 catalyst was proposed and the hypothesis about the Pd promotion was discussed.

Keywords: Density function theory (DFT); In situ DRIFTS; Simulated spectra; Catalytic reaction mechanism

1. Introduction

Selective catalytic reduction (SCR) is an effective method for removing NO. Since the pioneering work of Iwamoto et al. [1] and Held et al. [2] reported some success using Cu/ZSM-5 catalyst for selective catalytic reduction of NO_x in lean burn conditions, several investigations have brought a lot of promising zeolitic and nonzeolitic materials to be considered for the hydrocarbons-SCR (HC-SCR). It is commonly accepted that alumina-supported silver (denoted Ag/Al_2O_3) catalyst is a candidate for practical use, because of it is relatively durable and inexpensive [3–11]. However, the NO_x conversion over Ag/Al_2O_3 is quite low at low temperatures range of 300–400 °C, which is a major disadvantage. Ag/Al_2O_3 catalyst by co-impregnating a small amount of Pd was effectively enhanced for the selective reduction of NO with C_3H_6 on our earlier report [12,13]. The additive effect of Pd on Ag/mordenite was also reported by Masuda et al. using $(CH_3)_2O$ as a reductant [14].

In our previous report [13], we proposed a possible reaction mechanism for the C_3H_6-SCR of NO_x on Ag-Pd/Al_2O_3 catalyst, there is still a limited understanding on the formation and configuration of intermediate involved in the reaction. The exact Pd promotion mechanism for C_3H_6-SCR over Ag-Pd/Al_2O_3 is also still not clear.

The aim of this work is to study the mechanism of C_3H_6-SCR over Ag-Pd/Al_2O_3 and investigate the role of Pd in the formation of surface intermediate structure.

2. Experimental

The Ag/Al_2O_3 (Ag metal loading: 5 wt.%), Ag-Pd/Al_2O_3 catalysts were prepared by an impregnation method described in our earlier paper [13]. In situ DRIFTS experiments were performed using a NEXUS 670-FTIR fitted with a smart collector and a MCT/A detector cooled by liquid N_2. The DRIFTS cell (Nicolet) was equipped with CaF_2 and a heating cartridge that allowed samples to be heated up. Prior to each experiment, the catalyst was heated in the flow of 10 vol% O_2/N_2 for 60 min at 600 °C, then cooled to desired temperature for 30 min, and a spectrum of the catalyst in the flow of $N_2 + O_2$ serving as the background was recorded. All gas mixtures were fed at a flow rate of 100 ml/min, and all spectra were taken with a resolution of 4 cm^{-1} and an accumulation of 100 scans. Experimental spectra are plotted in Figs. 1 and 2.

* Corresponding author. Tel.: +86 10 62849123; fax: +86 10 62923563.
E-mail address: honghe@mail.rcees.ac.cn (H. He).

1386-1425/$ – see front matter © 2004 Elsevier B.V. All rights reserved.
doi:10.1016/j.saa.2004.11.040

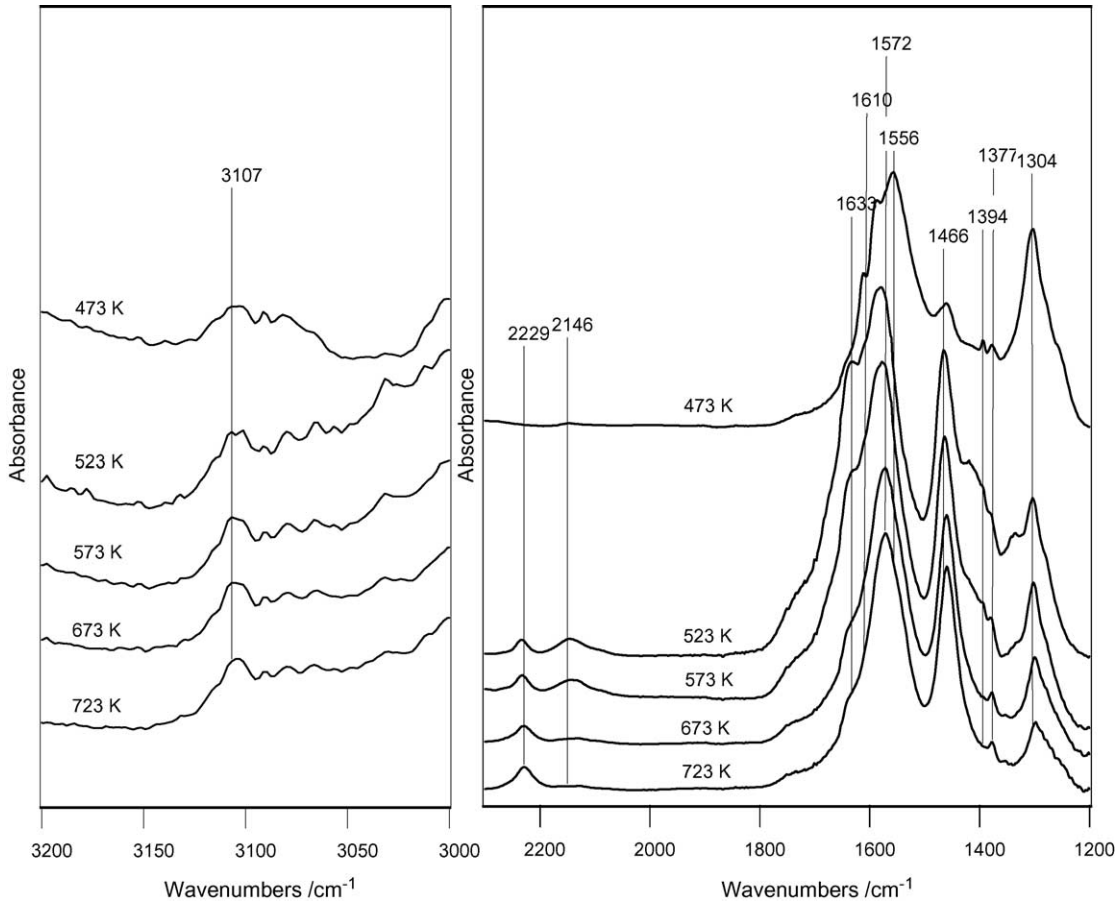

Fig. 1. In situ DRIFTS spectra of Ag/Al_2O_3 in a steady state at various temperatures in a flow of $C_3H_6 + O_2 + NO + N_2$. ($NO/C_3H_6/O_2/N_2$ = 800 ppm/1714 ppm/100,000 ppm/balance), total flow rate: 100 ml/min.

3. Theoretical

The density functional theory (DFT) calculations were carried out using Gaussian98 program. The properties of the calculated models (Fig. 3) were determined through the application of density functional theory using the B3PW91 gradient corrected functional (Becke's 3 parameter functional with the non-local correlation provided by the Perdew 91 expression). The 3-21G* basis set was used for all of the calculations. The calculated vibrational frequencies and intensities using Gaussian98 program are analyzed by the Hyperchem^{TM} Version 6.0 package.

4. Results and discussion

4.1. Experimental spectra

Fig. 1 showed in situ DRIFTS spectra of Ag/Al_2O_3 in a steady state at various temperatures in a flow of $C_3H_6 + O_2 + NO$. Many IR peaks appeared in the region between 1700 and 1300 cm^{-1}. According to the previous literature [6,15,16], the bands at 1304, 1556, 1610 cm^{-1} were attributed to bidentate nitrate, monodentate nitrate and bridge nitrate, respectively. The peaks at 1394 and 1377 cm^{-1} were attributed to $\delta(-CH_3)$, and $\delta(-CH_2)$ of the adsorbed acetate species. The peaks at 1572 and 1460 cm^{-1} were assigned to ν_{as} (COO) and ν_s (COO) of the adsorbed acetate [17,18]. The peak at 1633 may be associated with the frequencies of double bond stretching vibration, such as ν(C=C), ν(C=O). In general, stretching vibration frequencies of isolate C=C and C=O should be higher than 1633 cm^{-1}. An enolic species ($H_2C{=}CH{-}O\cdots M$) is a possible surface structure by partial oxidation of C_3H_6 over Ag/Al_2O_3. The conjugation of $H_2C{=}CH{-}O-$ group may induce the vibrational mode of C–C–O shifts to a frequency which is lower than ν(C=C) and higher than ν(C–O) [19]. As a consequence, the peak at 1633 cm^{-1} in Fig. 1 could be tentatively assigned to stretching vibration mode of enolic species (C=CH–O–) [11]. The band at 2229 could be attributed to an isocyanate (–NCO) species, which is a key intermediate species reported by many researchers [5,8,20]. The band at 2146 cm^{-1} was assigned to a –CN surface species [21]. With the increasing temperature, the peaks at 1304 and 1633 cm^{-1} disappeared gradually. Meanwhile, the peak at 2229 cm^{-1} reached the strongest intensity at 723 K. On the other hand, the bands at 1460 and

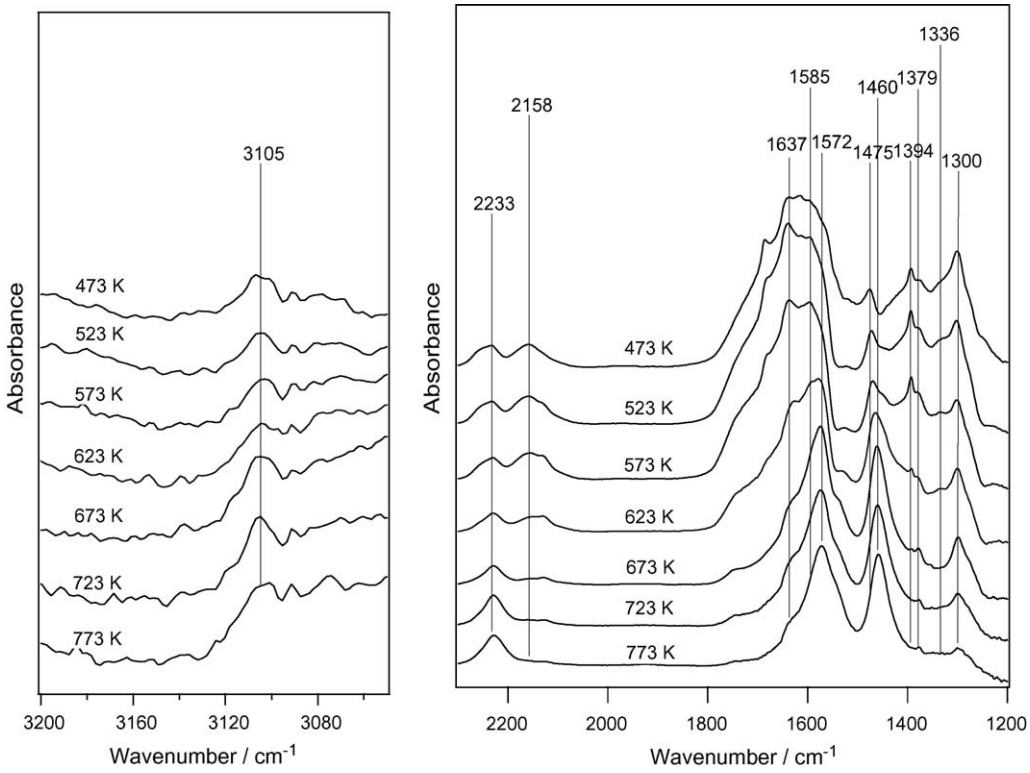

Fig. 2. In situ DRIFTS spectra of Ag-Pd/Al_2O_3 in a steady state at various temperatures. Feed: the same as the experiment shown in Fig. 1.

1572 cm^{-1} were still very strong. From these results we can speculate that the enolic species at 1633 cm^{-1} is very active to NO_3^-, while the activity of acetate is relatively weak in this reaction.

Fig. 2 showed in situ DRIFTS spectra of Ag-Pd/Al_2O_3 catalyst at the same conditions as the experiment shown as Fig. 1. Based on the comparison between Figs. 2 and 1, the band at 1637 cm^{-1} could be attributed to adsorbed enolic species [13]. Similarly, the bands at 1585 and 1300 cm^{-1} in Fig. 2 could be assigned to vibration mode of adsorbed monodentate nitrates and bidentate nitrates, the bands at 1572, 1460 and 1394 cm^{-1} in Fig. 2 could be attributed to the vibration mode of adsorbed acetate. The principal difference between Figs. 2 and 1 is the peak intensity on Ag-Pd/Al_2O_3 catalyst at 1637 cm^{-1} which is main peak at low temperature in Fig. 2. While, it is a shoulder peak in Fig. 1. With increased temperature, the bands of nitrate (1300 cm^{-1}) and enolic species (1637 cm^{-1}) decreased promptly, while the –NCO band (2233 cm^{-1}) progressively appeared. These results indicated that the enolic surface species is very active towards nitrate to form –NCO species. As a result, Ag-Pd/Al_2O_3 has a higher –NCO surface concentration than Ag/Al_2O_3 during the SCR of NO by C_3H_6. These results are in good agreement with activity of Ag/Al_2O_3 and Ag-Pd/Al_2O_3.

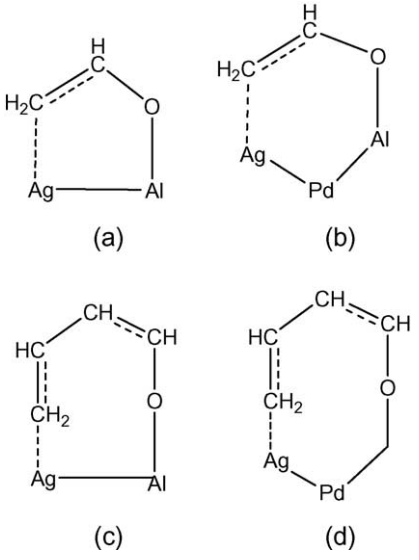

Fig. 3. Calculated models (a–d) for the reaction of enolic species on Ag-Pd/Al_2O_3 catalyst.

On the bases of DRIFTS (Figs. 1 and 2) and TPD-MS [22], we proposed the mechanism for the formation of absorbed enolic species over Ag/Al_2O_3 or Ag-Pd/Al_2O_3 catalyst in Scheme 1.

For the reaction (1) or (2), C_3H_6 is first catalytically oxidized to CH_3CHO, which then is adsorbed on Ag-Pd/Al_2O_3 catalyst to yield the ring structure, followed by decompose reaction to form NCO intermediate, and a further reaction of this compound finally leads to the formation of products (N_2, H_2O and CO_2).

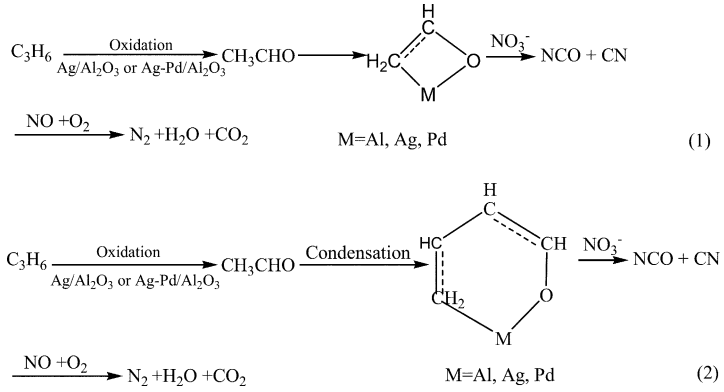

Scheme 1. Proposed reaction mechanism for the SCR of NO by C_3H_6 over Ag/Al_2O_3 or $Ag\text{-}Pd/Al_2O_3$ catalyst.

4.2. Calculation models and optimized structure

In order to investigate the structure of ring compound in reactions (1) and (2), we designed four calculated models. These models used in the calculation of the adsorption of enolic species on $Ag\text{-}Pd/Al_2O_3$ catalyst are shown in Fig. 3(a)–(d). The geometries of the four calculated models were fully optimized at DFT-B3PW91/3-21G* level. The optimized structures of the calculational models are plotted in Fig. 4(a)–(d). The optimized bond length and bond angle are marked in Fig. 4. From Fig. 4, the calculated value of the C=C bond length in enolic species for the models (a)–(d) is about 1.35–1.36 Å, which is within 1% of the experimental value of 1.34 Å. The C–C bond length in enolic species for models (d) determined from DFT calculations is about 1.44–1.45 Å. The optimized distance between the oxygen atom and the aluminum atom in the models (a)–(d) is about 1.75–1.77 Å. The optimized bond length for the Ag–Al bond in the models (a)–(d) is about 2.55–2.56 Å. The calculated equilibrium Ag–Pd bond length of the models (a)–(d) is about 2.60–2.61 Å. Dihedral angles for four calculated models in framework ring are significantly different. In these calculations, the dihedral angles, *D*(1,3,4,6), *D*(3,4,6,5) and *D*(4,6,5,1) for the framework ring of calculated model (a) are 53°, 3°, and −21°, respectively. Other dihedral data of the framework ring are also listed in Fig. 4. These dihedral angles show that framework ring is not planar.

4.3. Comparison of simulated and experimental spectra

Calculated vibration frequencies (in cm^{-1}) and IR intensity (in km/mol) and corresponding frequencies in the experimental spectra are listed in Table 1. The optimized geometries were taken as the basis for the calculation of IR frequencies by a normal coordinate analysis. Simulation spectra of Ag/Al_2O_3 and $Ag\text{-}Pd/Al_2O_3$ are presented in Fig. 5. From the analysis of animations of normal vibration modes it was clear that many vibrations have a high degree of mixing with other modes. Therefore, we provide in the following tentative assignments for only the intense spectral features in the vibrational spectra of the molecule based on the literature [23–29] and our simulated spectral analysis.

Table 1
Calculated vibration frequencies (in cm^{-1}) and IR intensity (in km/mol) for the calculated model at B3PW91/3-21G* level, and corresponding frequencies in the experimental gas-phase spectra

Model	Frequency	Intensity	Experiment	Vibration mode [23–29]
a	3144	25	3107 (Fig. 1)	CH_2 a-str.
	1626	35	1633 (Fig. 1)	CH_2=CH–O a-str.
	1471	17	1466 (Fig. 1)	CH_2 scis
	1365	8	1377 (Fig. 1)	CH bend
b	3140	23	3105 (Fig. 2)	CH_2 a-str.
	1611	44	1637 (Fig. 2)	CH_2=CH–O a-str.
	1466	16	1475 (Fig. 2)	CH_2 scis.
	1362	13	1394 (Fig. 2)	CH bend
c	3135	41	3107 (Fig. 1)	CH_2 a-str.
	1645	37	1633 (Fig. 1)	CH_2=CH–CH=CH–O a-str.
	1459	21	1466 (Fig. 1)	CH_2 scis.
	1361	22	1377 (Fig. 1)	CH bend
d	3136	32	3105 (Fig. 2)	CH_2 a-str.
	1652	82	1637 (Fig. 2)	CH_2=CH–CH=CH–O a-str.
	1493	18	1475 (Fig. 2)	CH_2 scis.
	1360	73	1394 (Fig. 2)	CH bend.

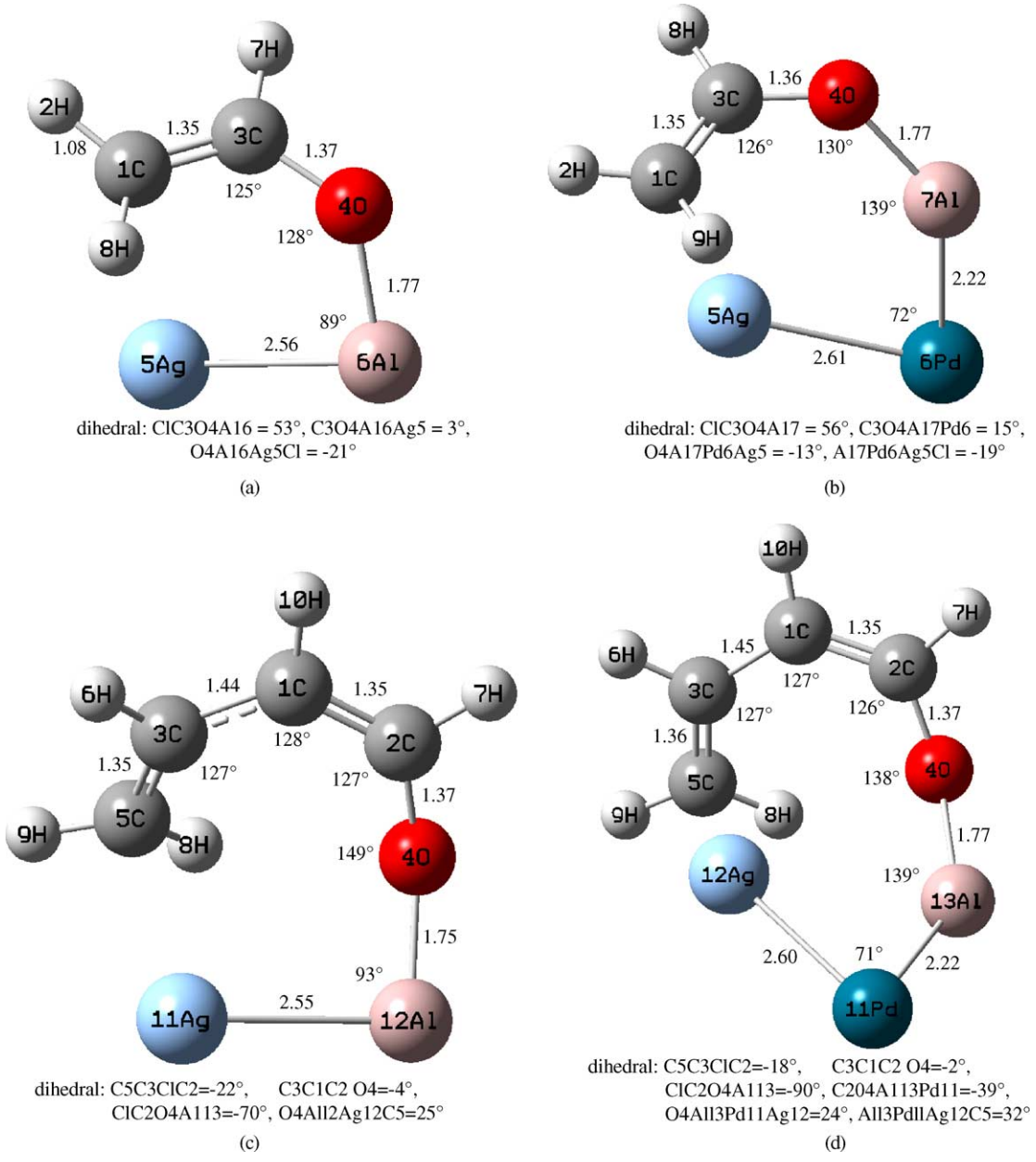

Fig. 4. Optimized configuration of calculation models for enolic species adsorption on Ag-Pd/Al_2O_3 catalyst.

For the reaction (1), the C=CH–O^- stretching frequency of model (a) (Fig. 4) was calculated at 1626 cm^{-1} with 35 km/mol intensity, which is similar to the experimental value 1633 cm^{-1} (Fig. 1). The calculated C=CH–O^- stretching frequency of model (b) (Fig. 5) at 1611 cm^{-1} with 44 km/mol intensity is 26 cm^{-1} lower than the experimental value (1637 cm^{-1}) (Fig. 1). The calculated C=CH–O^- stretching intensity of model (a) (35 km/mol) is weaker than the one of model (b) (44 km/mol), which is in agreement with the experiment (Figs. 1 and 2). The calculated CH_2 scissor mode of model (a) for the structure on Ag/Al_2O_3 catalyst at 1471 cm^{-1} with 17 km/mol intensity (Fig. 5) is close to the experimental value of 1466 cm^{-1} (Fig. 1). The calculated CH_2 scissor mode of model (b) for the structure on Ag-Pd/Al_2O_3 catalyst at 1466 cm^{-1} with 16 km/mol intensity is 9 cm^{-1} lower than the experimental value of 1475 cm^{-1} (Fig. 1). The CH bending vibration of model (a) was calculated at 1365 cm^{-1} with 8 km/mol intensity in the simulated spectrum of the structure (Fig. 5). This mode was observed at 1377 cm^{-1} in the infrared spectrum of the gas of the molecule (Fig. 1). The calculated CH bending vibration of model (b) (Fig. 5) at 1362 cm^{-1} with 13 km/mol intensity is 32 cm^{-1} lower than the experimental value of 1394 cm^{-1} with the weak intensity (Fig. 1).

For the reaction (2), the calculated frequency band at 1645 cm^{-1} of model (c) assigned to the CH_2=CH–O stretching vibration mode (Fig. 5) is in agreement with the experimental value of 1633 cm^{-1} for the enolic species

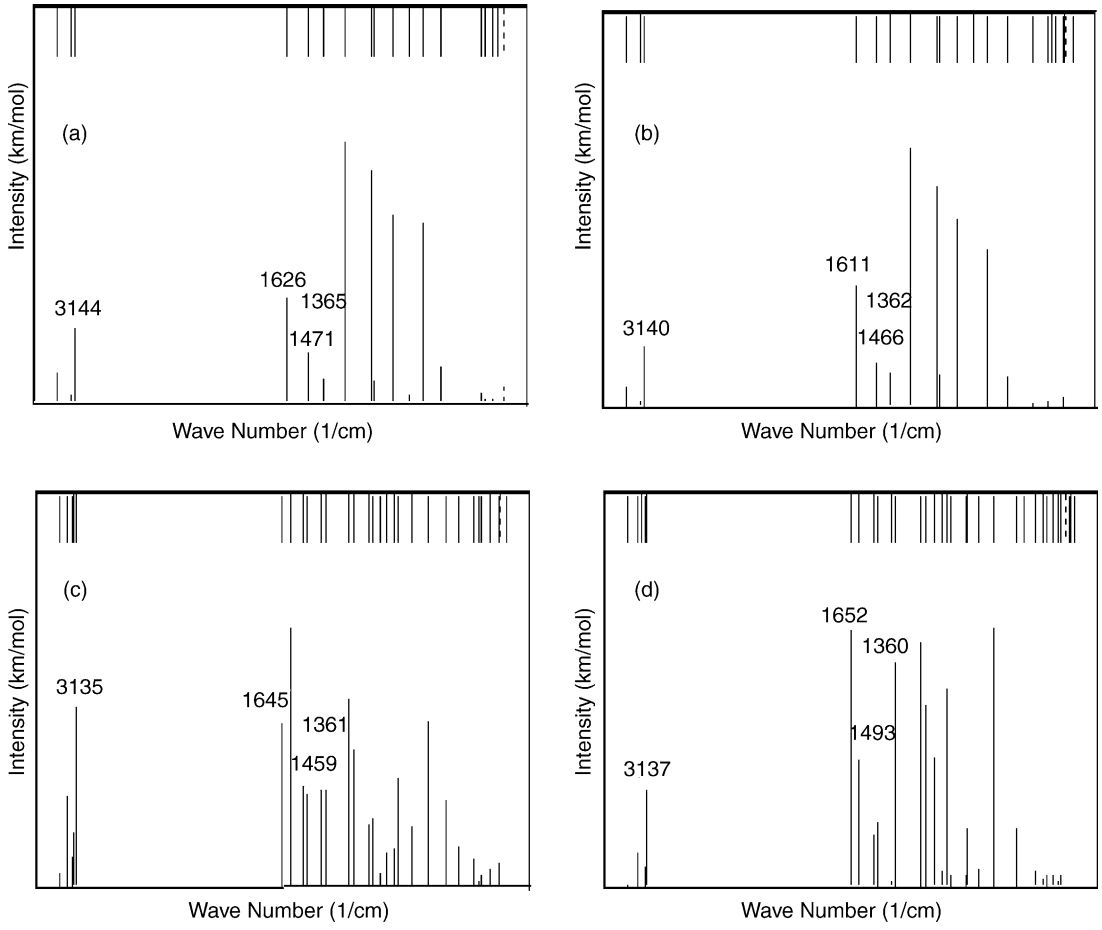

Fig. 5. Calculated vibrational IR spectra for the models (a–d) at DFT-B3PW91/3-21G* level.

adsorbed on the Ag/Al_2O_3 catalyst (Fig. 1). The calculated CH_2=CH–O stretching frequency of model (d) (Fig. 5) at 1652 cm^{-1} with 82 km/mol intensity is 15 cm^{-1} higher than the experimental value of 1637 cm^{-1} (Fig. 2). The calculated CH_2=CH–CH=CH–O stretching intensity of model (c) (37 km/mol) is weaker than the one of model (d) (82 km/mol), which is in agreement with the experiment (Figs. 1 and 2). The calculated CH_2 scissor mode of model (c) for the structure on Ag/Al_2O_3 catalyst at 1459 cm^{-1} with 21 km/mol intensity (Fig. 5) is close to the experimental value of 1466 cm^{-1} (Fig. 1). The calculated CH_2 scissor mode of model (d) for the structure on $Ag\text{-}Pd/Al_2O_3$ catalyst at 1493 cm^{-1} with 18 km/mol intensity is 18 cm^{-1} higher than the experimental value (1475 cm^{-1}) (Fig. 1). The CH bending vibration of model (c) was calculated at 1361 cm^{-1} with 22 km/mol intensity in the simulated spectrum of the structure (Fig. 5). This mode was observed at 1377 cm^{-1} in the infrared spectrum of the molecule (Fig. 1). The calculated CH bending vibration of model (d) at 1360 cm^{-1} with 73 km/mol intensity (Fig. 5) is 34 cm^{-1} lower than the experimental value of 1394 cm^{-1} (Fig. 1).

The most important additive effect of Pd on Ag/Al_2O_3 was that the calculated intensity of the CH_2=CH–O and CH_2=CH–CH=CH–O stretching vibrations mode increase, which is in agreement with the experiment. The calculations show clearly that the calculated IR spectrum for model (a) and (b) are closer to the corresponding experimental spectrum than model (c) and (d), respectively.

5. Conclusion

We have investigated the additive effect of co-impregnating a small amount of Pd in Ag/Al_2O_3 catalyst by means of DRIFTS and density functional calculations. The calculated IR spectra are in good agreement with experimental ones. The calculated results show clearly that simulated spectra with density functional theory quantum mechanical method can be considered as the advantageous auxiliary tool for analyzing the mechanism of the enolic species adsorption on Ag/Al_2O_3 or $Ag\text{-}Pd/Al_2O_3$ catalyst. Therefore, we conclude that the calculated models (a) and (b) are the reasonable models for investigating the reaction mechanism of the enolic species adsorption on Ag/Al_2O_3 or $Ag\text{-}Pd/Al_2O_3$ cluster. Reaction (1) is the most possible way for the enolic species adsorption on these catalysts.

Acknowledgements

This work was financially supported by the National Science Foundation of China (NSFC, Grants 20437010) and State Hi-tech Research and Development Project of the Ministry of Science and Technology, Peoples Republic of China (Grant 2003AA643010).

References

[1] M. Iwamoto, H. Yahiro, S. Shundo, Y. Yu-u, N. Mizuno, Appl. Catal. 69 (1991) 15.
[2] W. Held, A. Köenig, T. Richiter, L. Puppe, SAE paper (1990) 900496.
[3] T. Miyadera, K. Yoshida, Chem. Lett. 3 (1993) 1483;
T. Miyadera, Appl. Catal. B 2 (1993) 199.
[4] K.A. Bethke, H.H. Kung, J. Catal. 172 (1997) 93.
[5] K. Shimizu, H. Maeshuma, A. Satsuma, T. Hattori, Appl. Catal. B 18 (1998) 163.
[6] S. Sumiya, H. He, A. Abe, N. Takezawa, K.J. Yoshida, J. Chem. Soc., Faraday Trans. 94 (1998) 2217.
[7] S. Sumiya, M. Saito, H. He, Q.-C. Feng, N. Takezawa, Catal. Lett. 50 (1998) 87.
[8] F.C. Meunier, J.P. Breen, V. Zuzaniuk, M. Olsson, J.R.H. Ross, J. Catal. 187 (1999) 493.
[9] F.C. Meunier, V. Zuzaniuk, J.P. Breen, M. Olsson, J.R.H. Ross, Catal. Today 59 (2000) 287.
[10] Y. Yu, H. He, Q. Feng, H. Gao, X. Yang, Appl. Catal. B 49 (2004) 159.
[11] Y.B. Yu, H. He, Q.C. Feng, J. Phys. Chem. 107 (2003) 13090–13092.
[12] H. He, N. Irite, K. Onai, K. Yoshida, in: Proceedings of the 69th Annual Meeting of Chemical Society of Japan, A314.
[13] H. He, J. Wang, Q. Feng, et al., Appl. Catal. B 46 (2003) 365–370.
[14] K. Masuda, K. Shinoda, T. Kato, K. Tsujimura, Appl. Catal. B 15 (1998) 29.
[15] M. Haneda, Y. Kintaichi, M. Inaba, H. Hamada, Appl. Surf. Sci. 121–122 (1997) 391.
[16] T. Tanaka, T. Okuhara, M. Misono, Appl. Catal. B (1994) 4.
[17] K. Shimizu, J. Shibata, H. Yoshida, A. Satsuma, T. Hattori, Appl. Catal. B 30 (2001) 151.
[18] K. Shimizu, H. Kawabata, A. Satuma, T. Hattori, Appl. Catal. B 19 (1998) 87.
[19] Standard IR Spectra, Sadtler Research Labs.
[20] S. Kameoka, Y. Ukisu, T. Miyadera, Phys. Chem. Chem. Phys. 2 (2000) 367.
[21] K. Shimizu, H. Kawabata, H. Maeshima, A. Satuma, T. Hattori, J. Phys. Chem. B 104 (2000) 2885.
[22] Y.B. Yu, H.W. Gao, H. He, Catal. Today 93–95 (2004) 805.
[23] T. Shimanouchi, Tables of Molecular Vibrational Frequencies Consolidated Volume I, National Bureau of Standards, 1972. pp. 1–160.
[24] Y. Koga, T. Nakanaga, K. Sugawara, A. Watanabe, M. Sugie, H. Takeo, S. Kondo, C. Matsumura, J. Mol. Spectrosc. 145 (1991) 315.
[25] D.-L. Joo, A.J. Merer, D.J. Clouthier, J. Mol. Spectrosc. 197 (1999) 68.
[26] M. Hawkins, L. Andrews, J. Am. Chem. Soc. 105 (1983) 2523.
[27] M. Rodler, C.E. Blom, A. Bauder, J. Am. Chem. Soc. 106 (1984) 4029.
[28] S. Saito, Chem. Phys. Lett. 42 (1976) 399.
[29] M. Rodler, A. Bauder, J. Am. Chem. Soc. 106 (1984) 4025.